Rare Met. (2018) 37(12):1076–1081
https://doi.org/10.1007/s12598-018-1178-8

RARE METALS
www.editorialmanager.com/rmet

Synthesis and densification of zirconium diboride prepared by carbothermal reduction

Tao Gui, Xing-Ming Wang*, Lei Yang, Yu-Yang Liu, Xue Bai, Li-Jun Wang, Bo Song

Received: 7 May 2018 / Revised: 14 July 2018 / Accepted: 25 October 2018 / Published online: 20 November 2018

Abstract Using boron powder as additive, the preparation of zirconium diboride (ZrB_2) by carbothermal reduction was investigated. The results show that the carbothermal reduction cannot be completely done until the temperature is more than 1900 °C. The ZrB_2 particles prepared without boron (B) additive at 1900 °C for 3 h are rodlike and show a preferential grain growth along [001] direction. B additive changes the heat effect of the raw materials. With B additive, the morphology of ZrB_2 particles turns to be regular shape. The average particle size is about 3.6 μm with 2.5 wt% B additives. With more B additive, the shape of particles turns to be round like and the average particle size is decreased to 2.3 μm when 5 wt% B is added. The existence of oxides in grain boundary is a key factor to keep ZrB_2 ceramic from deep densification. Using ZrB_2 powder prepared with 5 wt% B additives, by controlling carbon content in ZrB_2 powder, ZrB_2 ceramic with 93% relative density is hot-pressed.

Keywords Zirconium diboride; Carbothermal reduction; Grain growth; Morphology control; Deep densification

1 Introduction

Zirconium diboride (ZrB_2) is widely used as ultra-high-temperature ceramics (UHTCs), electrode material, thermowell tubes, etc. [1–3]. The investigations on preparation and densification of ZrB_2 are always hot spots. There are many methods to prepare ZrB_2 powder including carbothermal reduction [4, 5], borothermal reduction [6, 7], self-propagating high-temperature synthesis (SHS) [8, 9], solution-based methods [10–12], etc. Carbothermal reduction attracts a lot of attention because of its uncomplicated and low-cost raw material [13]. Meanwhile, carbon, one of the raw materials of carbothermal reduction, is helpful for densification of boride ceramics because it can react with oxides existed in grain boundary [14, 15]. However, the particle prepared by carbothermal reduction is in micron size. In addition, the particle has a rod shape which makes it very difficult to be highly densified. Thus, the relative density of single-phase ZrB_2 ceramic sintered with ZrB_2 raw powder prepared by carbothermal reduction is very difficult to reach more than 90% [16–18] unless pretreatment such as attrition milling with raw powder is used or sintering additives are added [19–21] or nanometer-grade ZrB_2 powder is used [16]. However, the nanometer-grade powder is very costly, and the sintering additives may not be allowed in some applications like the integrated fuel burnable absorber (IFBA) ZrB_2 coating on the surface of UO_2 pellets in AP1000 reactor [22]. Furthermore, in IFBA ZrB_2 coating, boron is enriched with ^{10}B, which makes the preparation highly cost-sensitive. Therefore, it has great significance to develop a new technology to improve particle size and morphology of ZrB_2 powder prepared by carbothermal reduction so that highly densified ZrB_2 ceramic can be achieved. Combined solgel and carbothermal reduction [10–12] can well control the particle size and morphology of ZrB_2 powder. Unfortunately, solgel is costly and not easy to be industrialized.

Thus, in this paper, carbothermal reduction was used to prepare ZrB_2 powder, and its effect on particle size and

T. Gui, X.-M. Wang*, L. Yang, Y.-Y. Liu, X. Bai, L.-J. Wang
Division of Metallurgy and Materials for Rare Metals, General Research Institute for Nonferrous Metals, Beijing 100088, China
e-mail: mansionwang010@163.com

T. Gui, B. Song
School of Metallurgical and Ecological Engineering, University of Science and Technology Beijing, Beijing 100083, China

morphology was investigated. Also, the performance of densification of ZrB_2 powder was discussed.

2 Experimental

Zirconium oxide (ZrO_2) powder (> 99.5 wt%, 1–5 μm, China Nuclear JingHuan Zirconium Industry Co., Ltd), boric acid (H_3BO_3) powder (> 99.5 wt%, 50 μm, Sinopharm Chemical Reagent Co., Ltd) and graphite (C) powder (> 99.99 wt%, 5–10 μm, KAJET, Shanghai) were used as raw materials mixed in a certain proportion. C content in synthesized powder was controlled by adjusting the ratio of C powder in raw material. The carbothermal reaction in Reaction (1) was done with argon protection; for this reaction, $\Delta_r G_m^{\Theta} = -0.8157T + 1227.1$, where $\Delta_r G_m^{\Theta}$ is standard molar Gibbs free energy for chemical reactions and T is temperature.

$$ZrO_2(s) + B_2O_3(l) + 5C(s) \rightarrow ZrB_2(s) + 5CO(g) \quad (1)$$

Boron (B) powder (> 99.99 wt%, 20 μm, YFNANO, Shanghai) was used as an additive with the content of 2.5 wt% and 5.0 wt%. ZrB_2 powder was vacuum-hot-pressed at the temperature of 1980 °C and the pressure of 70 MPa with the holding time of 4 h.

The thermal effect of the raw materials was detected by thermal gravimetric analyzer (TGA/DSC1, Mettler Toledo). The phase structure was detected by X-ray diffractometer (XRD, D/max 2500, Rigaku, Japan). The particle size and morphology were analyzed by scanning electron microscope (SEM, JSM-6510, JEOL, Japan) equipped with energy-dispersive spectroscopy (EDS) for composition analysis. The relative density of ZrB_2 ceramic was analyzed by Archimedes method. The cross sections and grain of ZrB_2 ceramic were observed by transmission electron microscope (TEM, Tecnai G2 F20 S-TWIN, FEI, USA).

3 Results and discussion

3.1 DSC analysis of raw materials

Two kinds of raw materials were used in the experiments, with/without boron additive. Figure 1 displays DSC curves of the raw materials with 0 wt% and 2.5 wt% B additives, respectively. It can be seen that both DSC curves show two endothermic peaks at 112 and 163 °C, which are contributed to the removal of water absorbed and hydrated. Further, at around 1416 °C, both DSC curves show an endothermic peak which is probably resulted by the formation of ZrC or B_2O_2, as shown in Reaction (2)

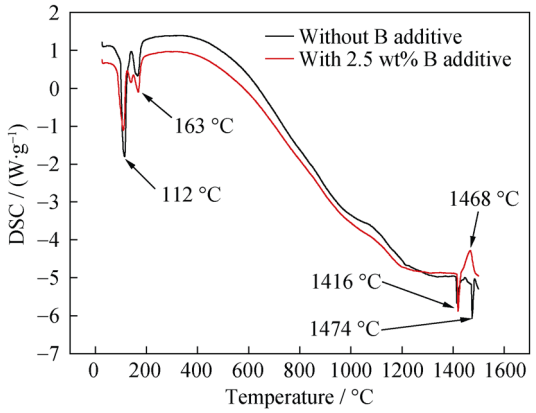

Fig. 1 DSC curves of raw materials under argon flow with a heating rate of 10 °C·min^{-1}

($\Delta_r G_m^{\Theta} = -0.3478T + 578.12$) and Reaction (3) ($\Delta_r G_m^{\Theta} = -0.3304T + 584.49$), respectively.

$$ZrO_2(s) + 3C(s) = ZrC(s) + 2CO(g) \quad (2)$$

$$B_2O_3(l) + C(s) = B_2O_2(g) + CO(g) \quad (3)$$

Li et al. [23] investigated the preparation of ZrC and reported that at a temperature more than 1127 °C, ZrC can be formed if $\lg(p_{CO}/p^{\Theta}) = -5$ (where p_{CO} is partial pressure of CO and p^{Θ} is standard pressure). Maeda et al. [24] investigated preparation of NbB_2 powder by carbothermal reduction and showed that at a temperature higher than 1277 °C, the formation of B_2O_2 gas in Reaction (3) maybe occurred.

Meanwhile, at temperature around 1470 °C, DSC curves in Fig. 1 show the contrary thermal effect. For the powder without B additive, it is endothermic, but for that with 2.5 wt% B, it is exothermic. Apparently, it reveals that different reactions happen when boron additive is used.

Figure 2 shows XRD pattern of the powder prepared by carbothermal reduction at 1450 °C. It can be seen clearly

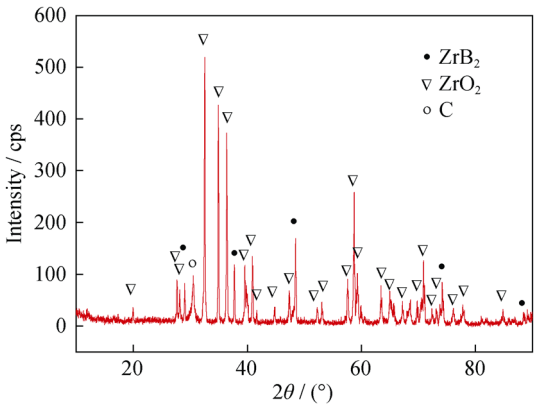

Fig. 2 XRD pattern of powder prepared by carbothermal reduction without B additive at 1450 °C

that ZrB_2 is formed and the carbothermal reduction reacts around 1450 °C. When boron is brought into raw materials, boron could be reacted with carbon to form B_4C at temperature around 1470 °C and a lot of heat is released at the same time, causing the formation of B_4C as shown in Reaction (4) ($\Delta_r G_m^{\Theta} = 0.0058T - 62.948$) which is exothermic reaction.

$$4B(s) + C(s) \rightarrow B_4C(s) \quad (4)$$

Therefore, although the carbothermal reduction is endothermic without B additive, the overall thermal effect becomes exothermic with 2.5 wt% B additives.

3.2 Effect of temperature on phase structure of carbothermal reaction

Figure 3 shows XRD patterns of ZrB_2 powders prepared at different temperatures. It can be seen that with the increase in temperature, the composition tends to be single phase of ZrB_2 gradually. The reaction is not completed from 1500 to 1800 °C; meanwhile, the phase content of ZrO_2 and C is diminished. At the temperature of 1900 °C, pure ZrB_2 is obtained.

The similar results are also reported. Khanra et al. [25] prepared ZrB_2 using ZrO_2–H_3BO_3–C system and found that B_4C and ZrC existed as minor phases with the temperature between 1500 and 1700 °C. Guo and Zhang [26] used ZrO_2–B_4C–C system to synthesize ZrB_2 powder and found that ZrC phase was formed with temperature between 1550 and 1650 °C. These results imply that quite a few subsidiary reactions exist during the process of carbothermal reduction reaction. The carbothermal reduction reaction cannot be completely done until the temperature reaches 1900 °C because of the kinetic factors and subsidiary reactions.

3.3 Particle size and its morphology control of ZrB_2

Figure 4 is SEM image of ZrB_2 prepared by carbothermal reduction at 1900 °C for 3 h. It can be seen that the particle is rodlike with the size of about 8 μm in length and 2–3 μm in diameter. It illustrates that the oriented grain growth is happened during the preparation. Yang et al. [27] reported that besides crystallographic properties, growth environment also had a great influence on preferential growth along [001] direction to form prism-like ZrB_2 particles. On the one hand, according to the periodic bond chain (PBC) theory [28], planes with a higher density of strong bonds (B–B > B–Zr > Zr–Zr) tend to grow faster along its normal direction than other planes in ZrB_2 cell [29]. On the other hand, the preferential growth along [001] direction proves that the crystal surface of (001) has lower surface energy which is consistent with the calculation reported by Liu [30]. Moreover, the vaporization of B_2O_3 possibly reduced the supersaturation of ZrB_2 nucleus and led to one-dimensional growth [31].

Figure 5 shows SEM images of ZrB_2 powder prepared with 2.5 wt% and 5.0 wt% B additives at 1900 °C by carbothermal reduction. It can be seen evidently that the particles are turned into regular shape, and no rodlike particles are found, compared to the particles prepared without B additive as shown in Fig. 4. Further, the mean particle size of ZrB_2 powder prepared with 5.0 wt% B is about 2.3 μm, which is smaller than 3.6 μm of ZrB_2 prepared with 2.5 wt% B.

As discussed in Sect. 3.1, boron additive could change the heat effect of the overall reactions. With the heat released by B_4C formation reaction, the environment of the formation of ZrB_2 nucleus is changed. Also, the extra heat source may reduce the reaction barrier of the carbothermal reduction reaction. Thus, with more boron additive, more heat is released, and the reaction rate of carbothermal reduction will be accelerated and lead to more ZrB_2 nuclei

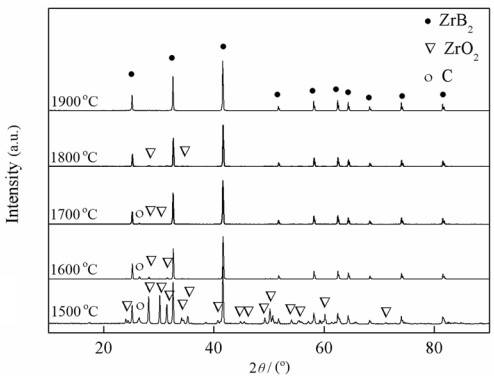

Fig. 3 XRD patterns of ZrB_2 powder prepared by carbothermal reduction at different temperatures

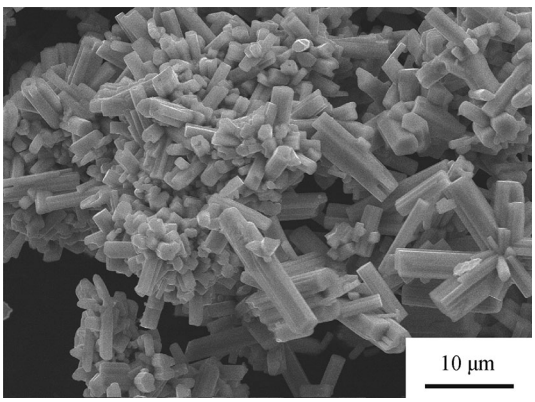

Fig. 4 SEM image of ZrB_2 prepared by carbothermal reduction without B additive at 1900 °C for 3 h

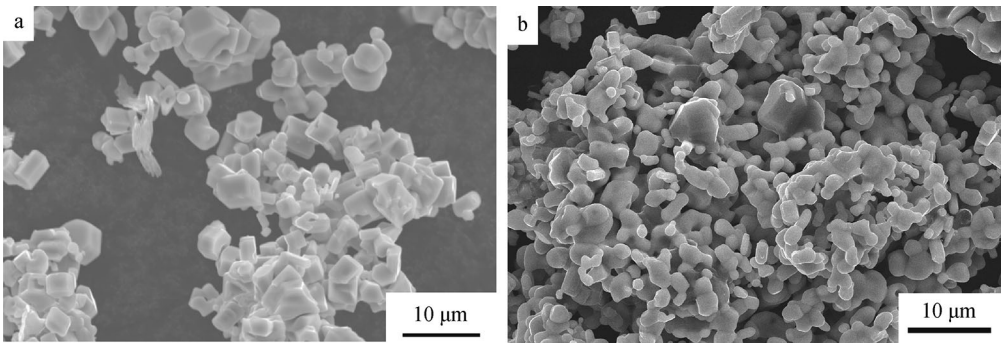

Fig. 5 SEM images of ZrB_2 prepared with **a** 2.5 wt% B additives and **b** 5.0 wt% B additives by carbothermal reduction

Table 1 ZrB_2 start powder and its hot pressing at 1980 °C with 70 MPa

No.	Additive content/wt%		Relative density/%	Remarks
	C	B		
1	0.15	0	78	Cracked
2	0.67	0	85	Good
3	0.28	2.5	90	Good
4	0.90	5.0	93	Good

formation. According to the theory of grain growth, more nuclei will be effective to promote grain refining. Finally, ZrB_2 particles become regular shape, and the size will be smaller with more B additives.

3.4 Densification of ZrB_2

It is well known that carbon is an effective additive to densify ZrB_2 ceramics because it can react with oxides existing in grain boundary of ZrB_2. In order to further illustrate the effect, four kinds of ZrB_2 powders were prepared with different carbon contents. Vacuum hot pressing was used to sinter ZrB_2 ceramic at the temperature of 1980 °C and the pressure of 70 MPa. The results are given in Table 1.

As given in Table 1, the relative density of ZrB_2 ceramics with the start powders prepared without B additive is less than 85%. By contrast, the relative density can be up to 93% when the ceramic was hot-pressed with the start powder prepared with 5.0 wt% B additives, which further illustrates that with boron additive, the sintering property of ZrB_2 powder is greatly improved.

Moreover, not only is the relative density of ZrB_2 ceramic hot-pressed with the start powder of No. 1 quite low (78%), but also the ceramic is cracked. TEM image (Fig. 6) shows that many holes exist in the ceramic body. And some particles are agglomerated near the boundary as shown in Spot A in Fig. 6. EDS result (Table 2) shows that there are some oxides, such as ZrO_2 or B_2O_3.

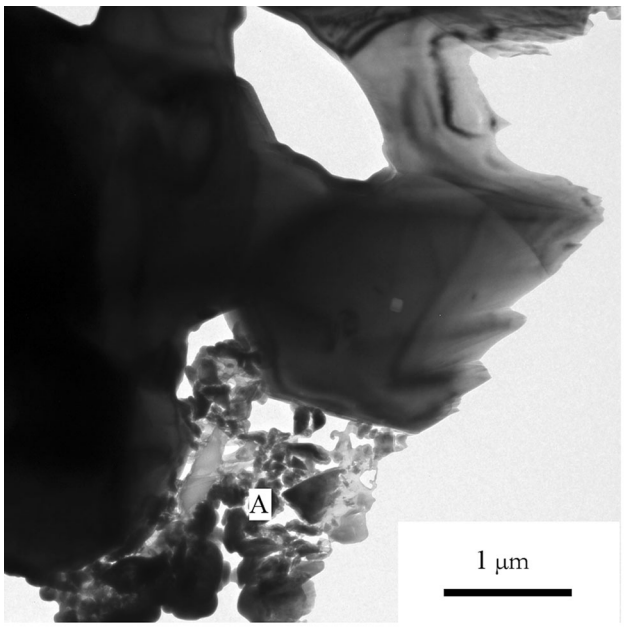

Fig. 6 TEM image of ZrB_2 ceramic hot-pressed with start powder of No. 1

Table 2 EDS result of hot-pressed ceramic with start powder of No. 1 (Spot A in Fig. 6)

Elements	*w*/wt%	*x*/at%
B	19.55	50.13
C	2.05	4.73
O	14.91	25.84
Zr	63.50	19.30

On the one hand, the presence of surface oxygen reduces the surface energy of the particle and prohibits the diffusion of the particles in the hot-pressing process [32]. On the other hand, the oxide impurities on the surface of the particle form channel between the grain boundaries to keep

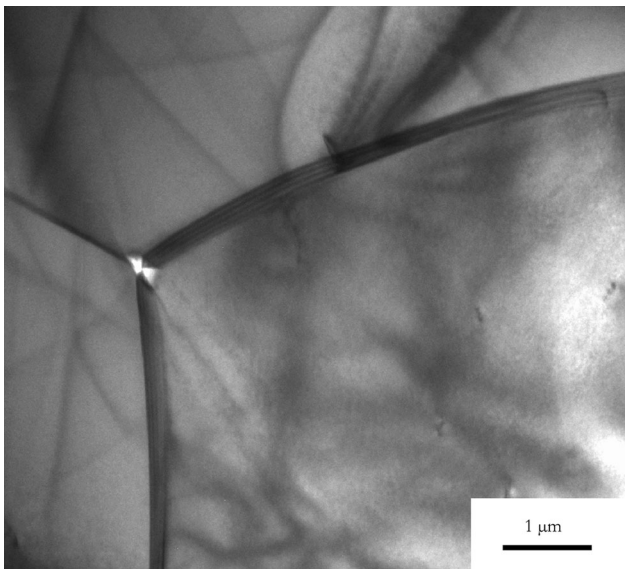

Fig. 7 TEM image of ZrB_2 ceramic hot-pressed with start powder of No. 4

from further densification [33]. In addition, the residual carbon in synthesized ZrB_2 powder can react with oxide impurities on the surface of ZrB_2 particles and resolve the aforementioned shortcomings [34–39].

Figure 7 shows TEM image of the ceramic hot-pressed with the start powder of No. 4. The relative density is 93%. It can be seen that the particles are packed together closely and no oxides are detected in grain boundary.

4 Conclusion

In this study, zirconium diboride (ZrB_2) powder was prepared with boron (B) additive by carbothermal reduction. The reaction cannot be completely done until the temperature reaches 1900 °C. The ZrB_2 grain shows a preferential growth along [001] direction. B additive can change the heat effect of raw materials and the morphology of final ZrB_2 particles. The morphology of final ZrB_2 particles is not rodlike; instead, it becomes regular. The final ZrB_2 particle size changes from 3.6 to 2.3 μm with the increase in B additives from 2.5 wt% to 5.0 wt%. The existence of oxides in ZrB_2 grain boundary is a key factor to keep ZrB_2 ceramic from getting deep densification. Single-phase ZrB_2 ceramic with 93% relative density is obtained by hot pressing using ZrB_2 powder prepared with 5 wt% B additives.

Acknowledgements This work was financially supported by the National Natural Science Foundation of China (No. 51674035).

References

[1] Fahrenholtz WG, Hilmas GE, Talmy IG, Zaykoski JA. Refractory diborides of zirconium and hafnium. J Am Ceram Soc. 2007;90(5):1347.
[2] Gasch MJ, Ellerby DT, Johnson SM. Ultra high temperature ceramic composites. In: Bansal NP, editor. Handbook of Ceramic Composites. New York: Springer; 2005; 197.
[3] Mroz C. Zirconium diboride. Am Ceram Soc Bull. 1995;74(6):164.
[4] Qiu H, Guo W, Zou J, Zhang GJ. ZrB_2 powders prepared by boro/carbothermal reduction of ZrO_2: the effects of carbon source and reaction atmosphere. Powder Technol. 2012;217(2):462.
[5] Jung EY, Kim JH, Jung SH, Choi SC. Synthesis of ZrB_2 powders by carbothermal and borothermal reduction. J Alloys Compd. 2012;538(42):164.
[6] Guo W, Zhang G. New borothermal reduction route to synthesize submicrometric ZrB_2 powders with low oxygen content. J Am Ceram Soc. 2011;94(11):3702.
[7] Guo WM, Tan DW, Zhang ZL, Xie H, Wu LX, Lin HT. Synthesis of fine ZrB_2 powders by new borothermal reduction of coarse ZrO_2 powders. Ceram Int. 2016;42(13):15087.
[8] Çamurlu HE, Maglia F. Preparation of nano-size ZrB_2 powder by self-propagating high-temperature synthesis. J Eur Ceram Soc. 2009;29(8):1501.
[9] La PQ, Han SB, Lu XF, Wei YP. Effects of the diluent content on microstructure of submicron ZrB_2 by combustion synthesis. J Inorg Mater. 2014;29(2):191.
[10] Ji G, Ji H, Li M, Li X, Sun X. Synthesis of zirconium diboride nano-powders by novel complex sol–gel technology at low temperature. J Sol–Gel Sci Technol. 2014;69(1):114.
[11] Cao YN, Du S, Wang JK, Zhang HJ, Li FL, Lu LL, Zhang SW, Deng XG. Preparation of zirconium diboride ultrafine hollow spheres by a combined sol–gel and boro/carbothermal reduction technique. J Sol–Gel Sci Technol. 2014;72(1):130.
[12] Ji H, Yang M, Li M, Ji G, Fan H, Sun X. Low-temperature synthesis of ZrB_2 nano-powders using a sorbitol modified sol--gel processing route. Adv Powder Technol. 2014;25(3):910.
[13] Graves JP, Chapman IT, Coda S, Johnson T, Lennholm M. Low temperature synthesis of ZrB_2 powder synergistically by borothermal and carbothermal reduction. Rare Met. 2011;30(1):548.
[14] Baik S, Becher PF. Effect of oxygen on the densification of TiB_2. J Am Ceram Soc. 2005;70(8):527.
[15] Zhu S, Fahrenholtz WG, Hilmas GE, Zhang SC. Pressureless sintering of carbon-coated zirconium diboride powders. Mater Sci Eng, A. 2007;459(1):167.
[16] He R, Zhang R, Pei Y, Fang D. Two-step hot pressing of bimodal micron/nano-ZrB_2 ceramic with improved mechanical properties and thermal shock resistance. Int J Refract Metals Hard Mater. 2014;46(1):65.
[17] Brochu M, Gauntt BD, Boyer L, Loehman RE. Pressureless reactive sintering of ZrB_2 ceramic. J Eur Ceram Soc. 2009;29(8):1493.
[18] Asl MS, Kakroudi MG, Nayebi B, Nasiri H. Taguchi analysis on the effect of hot pressing parameters on density and hardness of zirconium diboride. Int J Refract Metals Hard Mater. 2015;50:313.
[19] Wang H, Chen D, Wang CA, Zhang R, Fang D. Preparation and characterization of high-toughness ZrB_2/Mo composites by hot-pressing process. Int J Refract Metals Hard Mater. 2009;27(6):1024.

[20] Choi SK, Ui SW, Choi IS, Choi SC. Densification behavior of ZrB_2 with Co–WC as additives. J Ceram Soc Jpn. 2014;122(3):198.
[21] Chamberlain AL, Fahrenholtz WG, Hilmas GE. Pressureless sintering of zirconium diboride. J Am Ceram Soc. 2006;89(2):450.
[22] Wang Z, Zhang H, Gong S, Yao J, Ma SZ. Study on the IFBA pellets coating process. Nucl Sci Eng. 2015;35(4):633.
[23] Li R, Song S, Wang Y, Zhen Q. Preparation and thermodynamics mechanism of nanocrystalline ZrC powders. Chin J Rare Metals. 2015;39(7):605.
[24] Maeda H, Yoshikawa T, Kusakabe K, Morooka S. Synthesis of ultrafine NbB_2, powder by rapid carbothermal reduction in a vertical tubular reactor. Cheminform. 1994;215(1–2):127.
[25] Khanra AK, Pathak LC, Godkhindi MM. Carbothermal synthesis of zirconium diboride (ZrB_2) whiskers. Br Ceram Trans. 2007;106(3):155.
[26] Guo W, Zhang G. Reaction processes and characterization of ZrB_2 powder prepared by boro/carbothermal reduction of ZrO_2 in vacuum. J Am Ceram Soc. 2009;92(1):264.
[27] Yang BY, Li JP, Zhao B, Hu YZ, Wang TY, Sun DF, Li RX, Yin S, Feng ZH, Tang Q, Sato T. Synthesis of hexagonal-prism-like ZrB_2 by a sol–gel route. Powder Technol. 2014;256(1):522.
[28] Hartman P, Perdok WG. On the relations between structure and morphology of crystals. I. Acta Crystallogr. 1955;8(9):521.
[29] Fan Z, Guo Z, Cantor B. The kinetics and mechanisms of interfacial reaction in sigma fibre-reinforced Ti MMCs. Compos A Appl Sci Manuf. 1997;28(2):131.
[30] Liu GY. Monte carlo simulation for zirconium diboride ceramics during sintering initial stage. Harbin: Harbin Institute of Technology; 2008; 28.
[31] Zhao B, Yang BY, Wang TY, Sun DF, Hu YZ, Li RX, Yin S, Li JP, Feng ZH, Duan HP, Tang Q, Sato T. Nanocarbon-dependent synthesis of one-dimensional bead-chain-like β-SiC. Powder Technol. 2013;246:487.
[32] Zhang GJ, Zou J, Ni DW, Liu HT, Kan YM. Boride ceramics: densification, microstructure, tailoring and properties improvement. J Inorg Mater. 2012;27(3):225.
[33] Sciti D, Silvestroni L, Guicciardi S, Monteverde F. Reactive processes for Diboride-based ultra-high temperature ceramics. In: Fahrenholtz WG, Wuchina EJ, Lee WE, Zhou Y, editors. Ultra-High Temperature Ceramics: Materials for Extreme Environments. London: Wiley; 2014; 92.
[34] Sha JJ, Li J, Lv ZZ, Wang SH, Zhang ZF, Zu YF, Flauder S, Krenkel W. ZrB_2-based composites toughened by as-received and heat-treated short carbon fibers. J Eur Ceram Soc. 2017;37(2):549.
[35] Nisar A, Balani K, Sreenivas N, Ariharan S, Venkateswaran T. Effect of carbon nanotube on processing, microstructural, mechanical and ablation behavior of ZrB_2–20SiC based ultra--high temperature ceramic composites. Carbon. 2017;111:269.
[36] Nisar A, Balani K, Ariharan S. Synergistic reinforcement of carbon nanotubes and silicon carbide for toughening tantalum carbide based ultrahigh temperature ceramic. J Mater Res. 2016;31(6):682.
[37] Asl MS, Zamharir MJ, Ahmadi Z, Parvizi S. Effects of nano--graphite content on the characteristics of spark plasma sintered ZiB_2–SiC composites. Mater Sci Eng, A. 2018;716:99.
[38] Asl MS, Nayebi B, Ahmadi Z, Zamharir MJ, Shokouhimehr M. Effects of carbon additives on the properties of ZrB_2-based composites: a review. Ceram Int. 2018. https://doi.org/10.1016/j.ceramint.2018.01.214.
[39] Parvizi S, Ahmadi Z, Zamharir MJ, Asl MS. Synergistic effects of graphite nano-flakes and submicron SiC particles on the characteristics of spark plasma sintered ZrB_2 nanocomposites. Int J Refract Metals Hard Mater. 2018;25:89. https://doi.org/10.1016/j.ijrmhm.2018.03.017.